International Journal of Earth Sciences (2026) 115:48
https://doi.org/10.1007/s00531-026-02594-7

ORIGINAL PAPER

Occurrence and morphometric analysis of sorted bedforms on the Alentejo continental shelf, Southwestern Portugal

J. Noiva[1] · P. Brito[1] · M. Rosa[1] · C. Ribeiro[1,2] · P. Terrinha[1,3]

Received: 21 October 2025 / Accepted: 29 May 2026

Abstract

The distribution of detrital sediments across continental shelves can provide important information on mineral concentrations, geological processes, and ecosystem substrates. On the southwestern Portuguese continental shelf, this distribution is governed by a complex interplay of hydrodynamic energy gradients, seafloor morphology, and eustatic sea-level changes. In particular, the strong energy gradient from the coastline to the shelf break, combined with open-ocean-wave dynamics, tidal regimes, and active continental uplift, determines the specific nature and grain size of submarine deposits. To better understand these dynamics, this study employed continuously recording geophysical methods, including multibeam echosounder bathymetry and backscatter, complemented by ultra-high-resolution seismic profiling and sediment sampling. Our results reveal four distinct depositional environments: homogeneous fine-grained sediments near the shelf break, sorted bedforms on the flat outer shelf, isolated sorted bedforms on the mid-shelf, and a homogeneous sand sheet near the coast. Notably, the presence of isolated bedforms at depths exceeding 80 meters suggests they are generated by wave action, reflecting the long-term impact of the Holocene sea-level rise over the last 8,000 years and possibly active mobilization under modern hydrodynamic conditions. Consequently, these findings highlight how high-resolution mapping can reveal sediment patterns and environmental histories that remain hidden through traditional discrete sampling.

Keywords Isolated sorted bedforms · Seafloor acoustic mapping · Multibeam bathymetry · Backscatter · Ultra-high-resolution seismics

Introduction

Continental shelves of passive non-glaciated continental margins are frequently covered by sandy sediments deposited during sea-level rise, which often preserve two major types of large bedforms depending on the regional sediment supply. In high sediment-supply regions, features, such as sub-aqueous dunes or sand ridges predominate, as noted by Swift and Field (1981) and Xing et al (2012), whereas sediment-starved regions are characterized by "sorted bedforms" (SBs) or "rippled scour depressions". These terms were first proposed by Cacchione et al. (1984) to describe asymmetric rippled sandy seafloors with topographic reliefs of approximately 1 m height. In these systems, coarse sediment domains typically form in bathymetric lows, whereas fine sediment domains form bathymetric highs, creating distinct patterns that are well-illustrated by acoustic backscatter data (Murray and Thieler 2004; Goff et al. 2005). Although these features typically occur on inner continental shelves above 50 m water depth, their characterization remains essential for understanding the sedimentary architecture of starved margins.

The formation and temporal stability of sorted bedforms are governed by complex hydrodynamic processes and observations on their long-term evolution remain relatively scarce. Cacchione et al. (1984) originally attributed the formation of SBs to storm-induced, cross-shore downwelling flows, whereas other authors, such as Murray and Thieler (2004) and Goff et al. (2005), associate these with the influence of directional longshore currents. Studies on their stability have yielded varying results; for instance, Goff et al. (2005) found that while short-term displacements can be

✉ J. Noiva
joao.noiva@ipma.pt

1 Instituto Português do Mar e Atmosfera, Lisbon, Portugal

2 MARE—Marine and Environmental Sciences Centre, Lisbon, Portugal

3 Instituto Dom Luiz, Lisbon, Portugal

oscillatory, long-term morphology often indicates unidirectional movement. Conversely, Diesing et al. (2006) and Lo Iacono and Guillén (2008) have reported cases of stability on decadal timescales, with the latter suggesting long-term equilibrium based on surveys conducted 13 years apart. These diverse findings suggest that the behavior of SBs is highly dependent on the specific oceanographic and geological context of the shelf.

In this paper, we report the extensive occurrence of SBs on the sediment-starved mid-continental shelf of SW Portugal (Fig. 1), which differs significantly from the commonly reported depth limits. These bedforms occur between 120 m and 80 m below present-day sea level along a stretch of ~40 km, which makes these occurrences quite a novelty, because they are usually reported from water depths shallower than 50 m. By integrating original ultra-high-resolution seismic reflection data, multibeam bathymetry, and other acoustic backscatter methods together with seafloor samples, we discuss the origin and age of these features. Ultimately, this study provides new evidence on sediment transport at unusual depths on the mid-continental shelf and thereby challenges current models regarding the distribution of sorted bedforms on continental shelves.

Environmental settings/geological setting

The Iberian Peninsula is a large continental block situated at the junction of the Atlantic Ocean and Mediterranean Sea, north of the Nubia–Eurasia lithospheric plate boundary (Fig. 1). Its morphology is highly variable, characterized by high cordilleras, such as the Pyrenees, Betics, and the Central System, which are surrounded by extensive plains and long river systems. This complex topography, combined with the occurrence of strong NE Atlantic winds to Saharan air masses, results in a diverse climatic spectrum from humid sub-tropical to hot semi-arid conditions.

Significant vertical crustal movements and high-frequency seismicity have further shaped this margin, creating distinct morphological clusters and steep elevation gradients from the mountains to the coastline (Neres et al. 2018). These physiographic features have led to the formation of various submarine canyons with head scarps as shallow as 50 m, which act as efficient conduits for transferring the mobile nearshore sediment directly to the deep ocean. This process effectively inhibits substantial alongshore sediment transport and prevents the formation of a continuous, sustained sediment cover, leading to the characteristic sediment starvation of the shelf. Moreover, these conditions were further modulated by the rapid post-Last Glacial Maximum eustatic sea-level rise (since ~19 ka BP) across a shelf that varies significantly in width from 2 km to over 65 km.

The North Alentejo Continental Shelf (NACoS) is a specific sector of the West Iberia Margin, which originated as part of a rifted margin during the Mesozoic and was subsequently modified by magmatic and tectonic events. Post-rifting thermal subsidence was interrupted by Late Cretaceous Alkaline Magmatism (~94–72 Ma BP) and later by two phases of Alpine compression during the Eocene and Miocene. A key structural feature is the Arrábida fold and thrust belt, a ~600 m high and ~30 km long E–W trending structure that protects the NACoS coastline from dominant north-westerly winds and waves (Fig. 1). Finally, Pliocene–Quaternary glacial–eustatic variations overprinted the Neogene morphology, resulting in the erosion of the shelf, the progradation of sedimentary bodies (Terrinha et al. 2019), and the incision of the major submarine canyons that define the modern seafloor.

Continental shelf sediment sources

Systematic sampling of the Portuguese continental shelf (Instituto Hidrográfico 1985) for mobile sediment mapping (10-cm-deep samples spaced one nautical mile apart in the course of the SEPLAT Program in the period from 1974 to 2010), conducted under the SEPLAT Program between 1974 and 2010, has revealed quite continuous compositional patterns (Fig. S1 in the Supplementary Information). Inspection of these data demonstrates that the southern part of the Arrábida mountain range is surrounded by a narrow rim of sand, which widens considerably along the north–south NACoS coast, whereas distal sediments are classified as muddy silts and clays mixed with lithoclastic or bioclastic material. In addition, an elongated sand sheet extends parallel to the coast south of the Setúbal canyon, punctuated by scattered rocky outcrops of Mesozoic limestones and sandstones or Paleozoic metamorphic rocks. This sediment distribution is further influenced by coastal barriers, such as the Troia sand spit, which grew 7 km in the last 2 ky due to the attenuation of the Sado River's hydraulic capacity as the post-Last Glacial Maximum reached its maximum inundation level (Rebêlo et al. 2012).

The widespread occurrence of outcropping bedrock south of the Setúbal canyon at depths exceeding 100 m indicates that the mobile sediment cover is remarkably thin, generally less than 2 m in thickness (Fig. 1). North of the Setúbal canyon, the bedrock protrudes through the sediment cover even at shallower depths of approximately 30 to 40 m, confirming the sediment-starved nature of this shelf. The most significant exception to this thin cover is the Sado River ebb delta, which represents the thickest deposit in the area, reaching over 30 m (Brito 2009). Such starved-shelf settings, characterized by thin mobile sheets, are common along the west coast of Portugal, where sand wedges thicker than 5 to 10 m occur only sporadically above 50 m water depth (Mil-Homens et al. 2022).

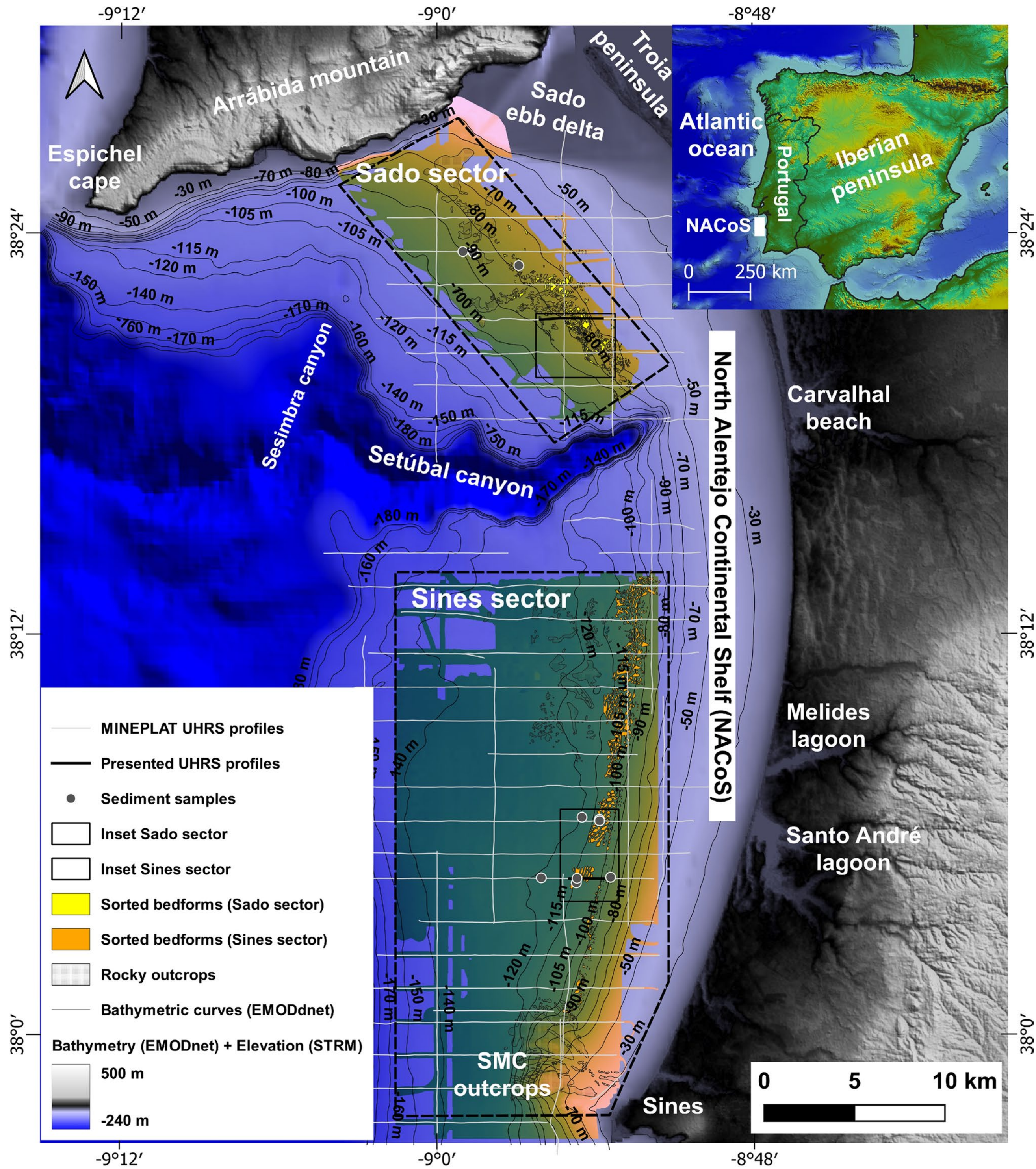

Fig. 1 Location of the study area showing the Northern Alentejo Continental Shelf (NACoS) off the western Portuguese coast. Bathymetric data are sourced from the European Marine Observation and Data Network (EMODnet) (EMODnet Bathymetry Consortium 2022), and elevation data from the Shuttle Radar Topography Mission (SRTM) (Farr et al. 2007). Black dashed polygons indicate the two sectors surveyed by multibeam echo sounder during the MINEPLAT project. Black boxes with bold lines define the areas presented in this paper. Inset: regional location of NACoS along the Iberian Peninsula, with bathymetry from the General Bathymetric Chart of the Oceans (GEBCO) (GEBCO Bathymetric Compilation Group 2022). The white rectangle in the inset outlines the study area. *NACoS* North Alentejo Continental Shelf; *EMODnet* European Marine Observation and Data Network; *SRTM* Shuttle Radar Topography Mission; *GEBCO* General Bathymetric Chart of the Oceans; *UHRS* ultra-high-resolution seismic; *SMC* Sines Magmatic Complex

Consequently, the sedimentary architecture of the NACoS is primarily defined by low sediment availability and the bypass conduits of major submarine canyons.

Wave regime

The Portuguese west coast is characterized by a high-energy wave climate, primarily driven by dominant north-westerly winds and swells. This regime exhibits significant seasonal variability, with average wave heights (Hs) exceeding 5 m during winter months and decreasing to approximately 2 m during the summer (Costa et al. 2001; Vitorino et al. 2002). During extreme storm events, significant wave heights can surpass 10 m with peak periods of 15 s, generating nearbed shear velocities at 80 m depth that can reach maximum values of 3.5 cm/s on the northern shelf (Vitorino et al. 2002). Applying linear wave theory to extrapolate these storm conditions down to the deeper limits of the shelf, the bottom orbital velocity amplitude reaches approximately 0.20 m/s at 100 m depth, yielding a corresponding nearbed shear velocity of ~2.25 cm/s. Long-term hydrographic data collected between 1988 and 2008 via the ONDMAR project further confirms this trend, showing that northwest swells account for 72.4% of occurrences at Leixões and 76.1% at Sines, as shown in Fig. S2 in the Supplementary Information (Costa and Esteves 2009). Consequently, the southern sector of the NACoS (Sines sector) follows the broader high-energy patterns typical of the West Iberia Margin.

In contrast, the northern area of the NACoS, specifically the Sado sector, displays a distinct wave climate due to the significant sheltering effect by the headland formed by the Arrábida mountain range (Fig. 1). This morphological barrier deflects the wave energy, causing the Sado sector to be primarily affected by southerly or westerly swells, regardless of the dominant offshore north-westerly orientation (Brito 2009). The resulting conditions are comparatively milder, with an Hs average of 1–2 m in summer and 2–4 m in winter, accompanied by shorter wave periods of 6–8 s. This protective influence is geographically constrained, gradually disappearing southwards as the coastline transitions back to the open-ocean conditions observed in the Sines sector. Thus, the localized topography of the Arrábida mountain range creates a distinctive hydrodynamic domain that differentiates the northern shelf from the Sines sector and the rest of the Portuguese western margin.

Materials and methods

Multibeam echosounder data

The multibeam echosounder data were acquired using a Reson T-50P multibeam system mounted on a side pole aboard the vessels RV Noruega and RV Diplodus. This system, capable of producing 512 individual acoustic beams with adjustable frequencies between 200 kHz and 420 kHz, allowed for high-resolution bathymetric surveys across a wide depth range on the continental shelf, from 5 to 250 m. Precise spatial positioning, vessel heading, and attitude were recorded using an Applanix POSMV Ocean Master system, which integrated two global navigation satellite system antennas and an inertial measurement unit, supported by real time kinematic corrections during most of the survey. In addition to bathymetry, the Reson T-50P recorded backscatter signals via the "Calibrated Snippets" option, which automatically balanced receiver gain according to water depth and operator-defined parameters. Although frequencies varied between 200 and 400 kHz using the continuous wave option, a 350 kHz frequency was typically selected to ensure data homogeneity throughout the study area.

The processing of the backscatter data was conducted using both Teledyne PDS software and the QPS FM Geocoder Toolbox, where calibrated snippets were utilized directly without the need for further external calibration. Within the FM Geocoder environment, the default parameters for the Reson T-50P were fine-tuned to match the actual acquisition values, and minor bias adjustments were applied to specific survey lines to enhance data consistency. The resulting mosaics were exported as tagged image file format images and subsequently refined within the Quantum GIS software (QGIS Development Team 2023). By carefully selecting maximum and minimum gray scale values, the individual mosaics were blended as seamlessly as possible to produce a continuous and high-quality representation of the seafloor acoustic properties.

Ultra-high-resolution seismic multichannel reflection data

The 2D ultra-high-resolution seismic multichannel reflection data were acquired using a Geo Marine Survey System, which integrates a 200-tip lightweight sparker sound source with a 24-channel single-element streamer featuring a 3.125 m group spacing and a 75 m active section. During the survey, both the source and receiver were towed at a depth of 0.3 m with a near offset of 3 m, while the spreading geometry and positioning were continuously monitored by a differential global navigation satellite system utilizing three double antennas mounted on the source and streamer buoys. Data acquisition parameters were carefully calibrated, employing an energy setting of 400 J (2 J per tip), a trigger rate of 2 Hz, and a sampling rate of 10,000 Hz (0.1 ms sample size) within a 500 ms recording window. This precise instrumental setup ensured the collection of high-density acoustic data necessary for detailed sub-bottom profiling of the continental shelf.

The subsequent post-processing of the seismic data was conducted using RadExPro software, involving a comprehensive sequence of steps to optimize image quality and resolution. This workflow included denoising, predictive deconvolution, and offset estimation correction by direct arrival picking, followed by static residuals correction using common offset spatial averaging as described by Duarte et al. (2017). Further refinements were achieved through interactive velocity analysis, normal move-out correction, trace stacking, and post-stack Kirchhoff time migration-, complemented by zero-offset multiple attenuation and tidal corrections. As a result, the final seismic sections exhibit a central mean frequency between 800 and 1200 Hz, providing an average vertical resolution of 0.25 to 0.40 m and a signal penetration below the seabed ranging from 35 to 150 m.

Sediment analysis

Sediment sampling

Surface sediment samples were collected on an irregular grid across the Alentejo continental shelf using a Smith–McIntyre grab sampler, which possesses an approximate maximum sampling capacity of 5,000 cm^3 at a 25 cm penetration depth. For this study, ten specific sediment samples located in the Sado and Sines sectors (Fig. 1) were selected and analyzed with the primary goal of calibrating the acoustic backscatter data. While this equipment is highly effective for recovering particles larger than fine-grained sand, it is important to note that a portion of the fine-grained sand and most of the finer sediment fraction can be lost during the recovery process. Once on board, these surface samples were immediately photographed, described, and subsampled for refrigerated storage. This rigorous protocol continued onshore, where the samples were maintained in refrigerated conditions until they were opened for final laboratory description, photography, and grain-size analysis. Consequently, this integrated sampling and storage workflow ensured that the physical characteristics of the sediments were accurately preserved for comparison with the geophysical data.

Grain-size analysis

The sediment subsamples selected for grain-size analysis underwent a rigorous preparation process involving washing with 40% hydrogen peroxide to remove organic matter, followed by drying at 100°C. To ensure representative results, the total dried sample was quartered to obtain splits of approximately 500 g, while aggregated particles were carefully crushed (disaggregated) using a rubber-coated mortar and pestle to avoid altering individual grain dimensions. The samples were then weighed and processed through an analytical sieve shaker for 20 min, using a stack of five stainless-steel sieves ranging from 63 µm (4 phi) to 2.0 mm (−1 phi) at 1-phi intervals; however, it should be noted that silt- and clay-sized particles were not recovered during the initial sample collection. Textural parameters, including mean grain size, standard deviation, skewness, and kurtosis, were subsequently calculated using both percentile and moment methods using the GRADISTAT statistical package of Blott and Pye (2001). This analytical framework, based on Folk's textural classification (Folk 1954) and the Udden–Wentworth scales (Udden 1914; Wentworth 1922), enabled for a precise physical characterization of the shelf sediments.

GIS data analysis

The study of depositional and erosional seabed features allows for the inference of both qualitative and quantitative environmental conditions based on their specific morphologies. While some features exhibit simple, regular boundaries, others possess convoluted and complex outlines, making it challenging to quantitatively capture their characteristics with a single attribute (Liu et al. 2010). To address this, a comprehensive characterization of sorted SB shapes was performed by calculating planimetric attributes, including perimeter, area, and minimum bounding rectangle, alongside specific shape indices, such as orientation, elongation, compactness, and rectangularity. The orientation/azimuth is the angle between the reference direction and the major axis of the best-fit ellipse. The elongation index, defined as the ratio between the length and width of the minimum bounding rectangle, indicates maximal elongation as it approaches zero, whereas the compactness index, also known as the Polsby–Popper score, compares the feature's area to that of a circle with the same perimeter. A score of zero indicates a complete lack of compactness and a score of one indicates maximal compactness (a circle). Furthermore, the rectangularity index evaluates the similarity of an object to a rectangle by comparing its area to that of its minimum bounding rectangle. Together, these metrics provide a robust geometric framework for distinguishing between different bedform morphologies.

Complementing these planimetric measurements, the sinuosity of linear shapes was evaluated by applying the centreline attributes technique. This method analyses the geometric relationship of a centreline with respect to the feature boundaries, providing a detailed assessment of shape complexity (Nyberg et al. 2015). All spatial calculations and geometric analyses were performed within the QGIS environment (QGIS Development Team 2023). Specifically, the planimetric and geometric attributes were derived using the NeatMap toolbox (Brasebin et al. 2019), while the centreline attributes were processed using the Geometric Attributes toolbox (Nyberg et al. 2015). By integrating these diverse GIS tools, the study ensures a highly precise and reproducible quantification of the seafloor's geomorphological patterns.

Results

Seabed morphology

The NACoS shelf is limited onshore by the Arrábida Mountain to the north and the sandy coastline of Carvalhal beach and the Sines magmatic complex to the east (Fig. 1). A dominant feature of this shelf is the Setúbal canyon, which possesses a head scarp at −50 m and extends for approximately 140 km toward the Tagus abyssal plain at −4500 m water depth, dissecting the NACoS in two distinct sectors. This physiographic division is crucial for understanding the regional sediment transport, as the canyon serves as a major structural boundary that influences the bathymetric contours and the overall continental shelf architecture.

The northern sector, or the Sado sector, exhibits a roughly triangular geometry defined by the Arrábida Mountain and the Troia peninsula (Fig. 1). In this area, the continental shelf width varies from over 20 km to about 3 km off Espichel cape, with the shelf break depth varying between −130 m and −160 m water depths at an average slope of 0.44º. Notably, the slope becomes irregular between −70 m and −80 m water depths, with steeper gradients occurring, where hard rock outcrops are present, as documented in profiles Sado 3 and Sado 4 (Fig. S4 and Table S1 in the Supplementary Information). Significantly, the SBs are concentrated within this −70 m to −80 m water depths range, where the slope gradient is lower than in adjacent intervals and situated upslope of a 7 m high escarpment.

The southern sector, or the Sines sector, extends for 35 km from the Setúbal canyon to Sines cape (Fig. 1), with a shelf width that narrows from 26 km to 14 km moving southwards. This sector presents a steeper average shelf slope of 0.60º, which increases toward the south, from 0.56º to 0.66º, as the shelf narrows, as illustrated in profiles Sines 2 and Sines 4 (Fig. S5 and Table S2 in the Supplementary Information). Here, the shelf break is positioned deeper than in the Sado sector, lying between −160 m and −180 m water depths. While the morphology is generally smooth, it becomes highly irregular off the Sines cape due to the outcrops of the Sines magmatic complex (Fig. 1), where coast-parallel bathymetric contours become wiggly below −90 m water depth.

Sorted bedform (SB) morphology

Sorted bedform (SB) types

The acoustic characterization of the seafloor is based on backscatter amplitude, where high-amplitude signals represent coarser-grained sediments with mean grain sizes ranging from very coarse gravelly sand (<-1.0 φ) to medium sand (>1.0 φ), whereas low-amplitude backscatter represents finer-grained sediments with mean grain sizes ranging from medium sand (>1.0 φ) to mud (>4 φ) (e.g., Goff et al. 2005; Liu et al. 2018), as shown elsewhere in this paper. In this study, SBs are identified as low-relief sedimentary features, typically less than 1 m high from crest to trough, occurring at the transition between high and low backscatter areas. These features are clearly discernible by a high-contrast black and white pattern in the backscatter maps (Fig. 2 and Fig. 3), allowing precise mapping of the boundary between different textural domains. Consequently, this acoustic contrast serves as the primary tool for delineating the spatial distribution and morphological complexity of the bedforms across the shelf.

Based on the analysis of distribution and shapes within this transition area (Fig. 2, Fig. 3, Fig. 4 and Fig. 5), three distinct types of sorted bedforms were identified: irregular sand patches or stripes (Type A), and two variations of Isolated Sorted Bedforms (ISBs) characterized by muddy sand bodies embedded in coarser sediment (Type B and Type C). Type A SBs (Fig. 4 and Fig. 5) are restricted to the deepest parts of the NACoS, appearing within the muddy sand domain at the base of slope breaks, typically between -80 m and -90 m water depths in the Sado sector and below -105 m to -115 m water depths in the Sines sector (Figs. S4 and S5 in the Supplementary Information). Moving landwards and upslope beyond this transition zone, where the seafloor sediment becomes progressively coarser, the ISBs begin to outweigh the Type A SBs, marking a significant shift in the depositional style of the continental mid-shelf.

Type B and Type C ISBs (Fig. 3 and Fig. 4) exhibit more complex geometries and are often intermingled, with their distribution being irregular and not solely dependent on water depth. Type B ISBs display a coherent linear orientation and consist of low elevation (< 2 m high) fine sediment bedforms with asymmetric flanks, featuring a gentle seaward-dipping slope and a steeper landward-dipping flank, with dimensions reaching up to 200 m in width and 1 km in length (e.g., Fig. 5). Type C ISBs, which appear as irregular or coalescent low-relief muddy sand forms, coexist with Type B until both types eventually disappear upslope as coarse sediments become ubiquitous above -70 m water depth in the Sado sector and −90 m

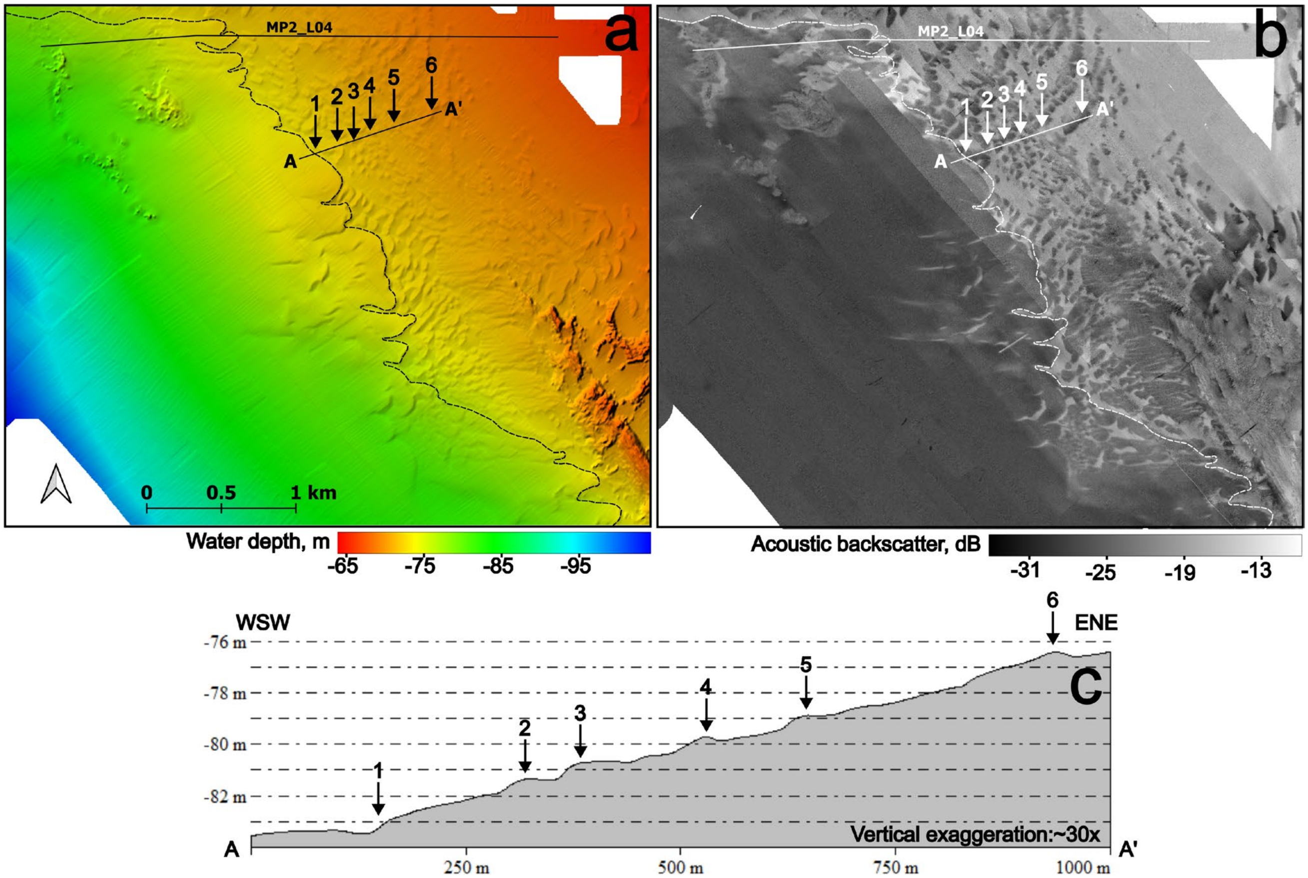

Fig. 2 Geomorphological and acoustic characterization of the Sado sector. **a** Multibeam bathymetry showing water depths ranging from –65 to –95 m. **b** Acoustic backscatter mosaic, where low intensity (dark gray, –31 dB) corresponds to finer sediments and high intensity (light gray, –13 dB) to coarser sediments. Dashed lines in **a** and **b** indicate the boundaries between these sediment facies. Hillshading in **a** and **b** is generated from an azimuth of 315° and an altitude of 45°. **c** Bathymetric profile along the A–A' transect (indicated in **a** and **b**) highlighting low-relief sorted bedforms (SB) numbered 1–6. Vertical exaggeration is ~30×. Profile orientation is West–Southwest (WSW) to East–Northeast (ENE), see Fig. 1 for the general location. *SB* sorted bedform; *dB*:decibels; *WSW* west–southwest; *ENE* east–northeast. Note that deeper than the dashed line the ISBs coexist with other types of SBs

water depth in the Sines sector. Thus, the transition from these isolated bedforms to a continuous coarse sediment sheet highlights the hydrodynamically forced nature of the mid-to-inner continental shelf boundary.

Spatial morphology of sorted bedforms (SBs)

The quantitative analysis of the plan view shapes of the SBs was conducted by calculating planimetric attributes for dimensions and shape attributes for geometry, specifically targeting ISBs of types B and C. Detailed statistics for these attributes are presented in Tables S3 and S4 in the Supplementary Information for the Sado and Sines sectors, respectively. Histograms of maximum length reveal that the Sines sector ISBs tend to be longer than those in the Sado sector, with 75% of observations in the Sines sector falling within the 0–250 m range (Fig. S6, left, in the Supplementary Information) compared to the 0–150 m range in Sado (Fig. S6, left, in the Supplementary Information). A similar trend is observed in maximum width, where both sectors show a modal interval of 0–40 m, but the Sines sector exhibits a higher percentage of wider forms (Fig. S7, right, in the Supplementary Information). These results indicate that while both sectors share a common dimensional base, the Sines sector facilitates the development of wider ISBs.

The orientation of the ISBs, as shown in the maximum elongation rose diagrams (Fig. 6), highlights significant regional differences in hydrodynamic influence. In the Sado sector (Fig. 6, left), the data show a large scatter with a mean azimuth of 105° and a modal interval (174°–162°) that aligns with the dominant wave direction of the western Portuguese coast, while the mean reflects the predominant west and southwest swells reported by Brito (2009). Conversely, the Sines sector (Fig. 6, right) exhibits a much better-constrained distribution, with 69% of observations aligned between 0° and 45° (N–S to NE–SW) and a prominent modal interval at

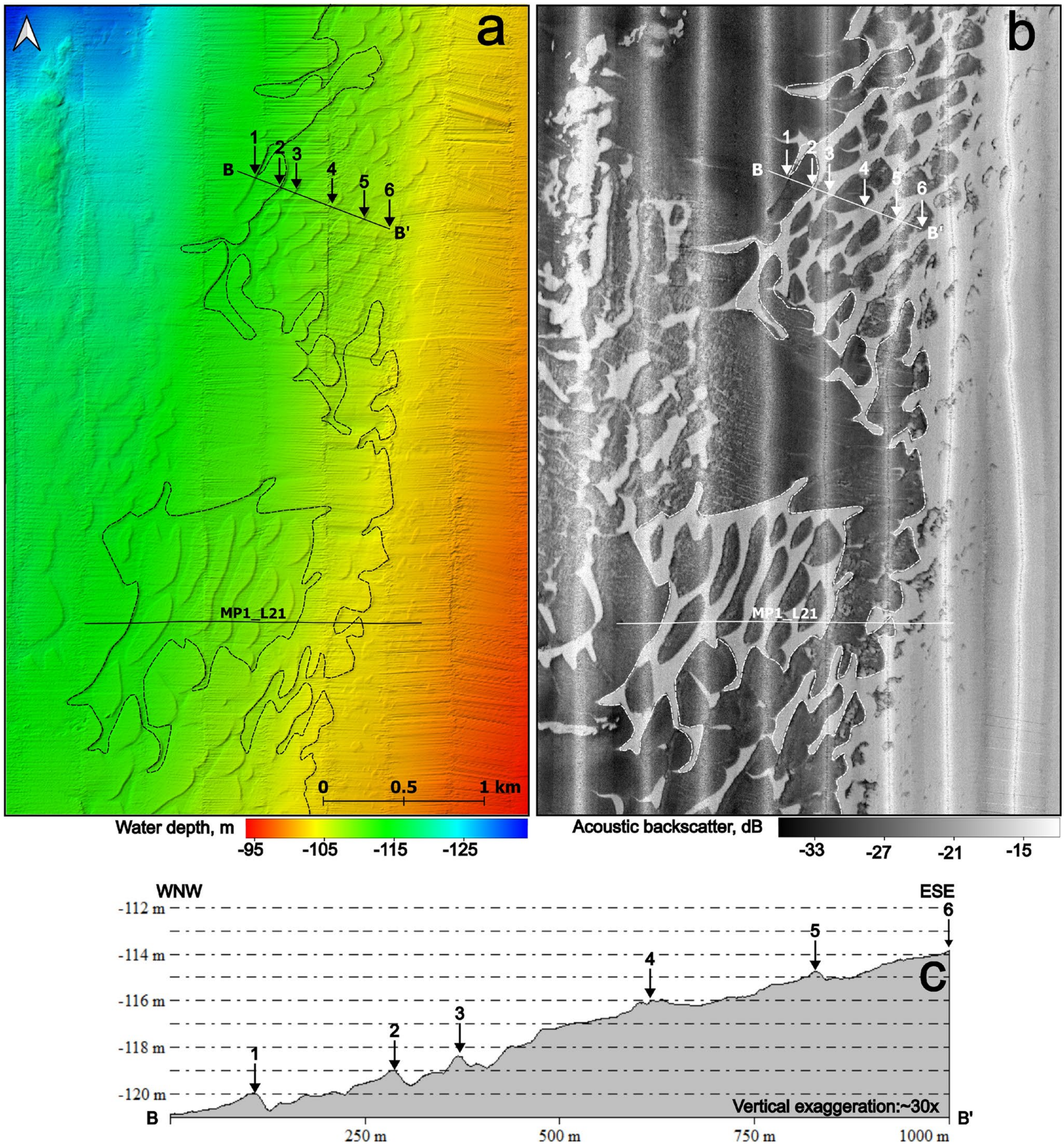

Fig. 3 Geomorphological and acoustic characterization of the Sines sector. **a** Multibeam bathymetry showing water depths from –95 m (orange) to –125 m (blue). **b** Acoustic backscatter mosaic ranging from –33 dB (dark gray/black) to –15 dB (light gray/white). Hillshading in **a** and **b** is generated with an illumination azimuth of 315° and an altitude of 45°. The black dashed line in **a** and the white dashed line in **b** delineate the boundaries between finer (low backscatter) and coarser (high backscatter) sediment facies. The V-shaped area of low backscatter between the two sorted bedform (SB) fields contains thin streaks of high backscatter material oriented perpendicular to the bedform elongation. c Bathymetric profile along the B–B' transect (indicated in a and b) showing low-relief sorted bedforms numbered 1 to 6. The morphological asymmetry suggests upslope migration toward the ESE. Vertical exaggeration is ~30×. Profile orientation is West–Northwest (WNW) to East–Southeast (ESE), see Fig. 1 for the general location. *SB* sorted bedform; *dB* decibels; *WNW* west–northwest; *ESE* east–southeast. Note that between the two groups of well-defined ISBs these display fuzzier outlines and coexist with other types of SBs

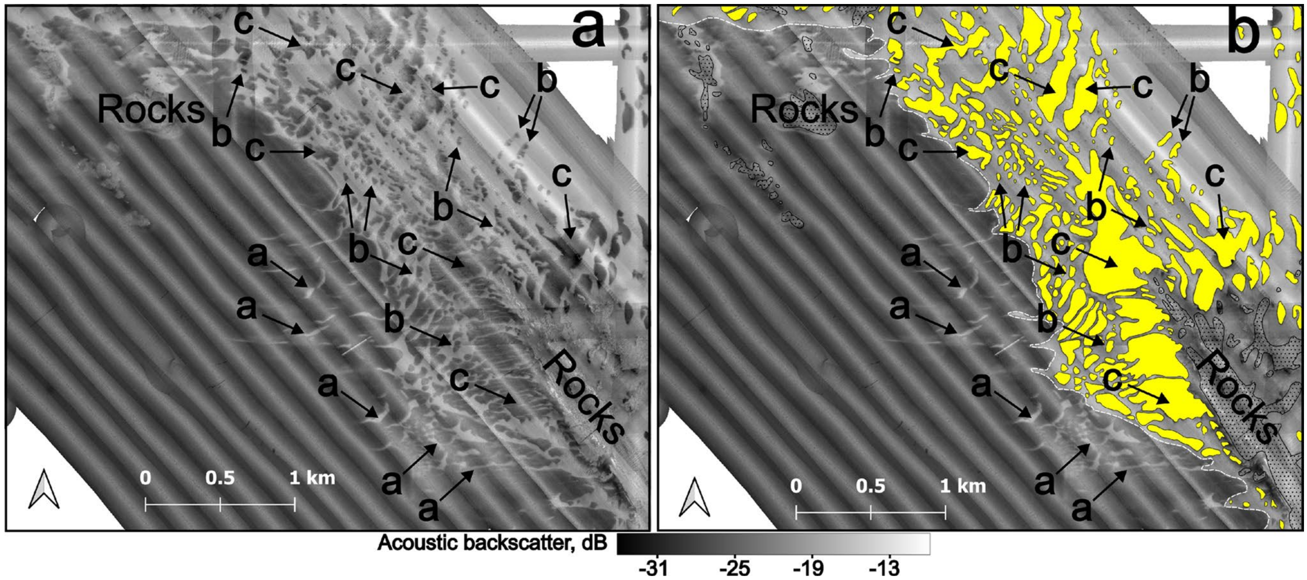

Fig. 4 Acoustic backscatter characterization of sorted bedforms in the Sado sector. **a** Backscatter mosaic illustrating the spatial distribution of the three identified sorted bedform (SB) types: Type A (**a**), Type B (**b**), and Type C (**c**). Fine sediments (low intensity, dark gray) dominate the seaward side, while coarse sediments (high intensity, light gray) are more prominent on the landward side. **b** Detailed interpretation of the sediment facies boundary (white dashed line), with Type B and Type C bedforms highlighted in solid yellow for enhanced visualization. Dotted polygons indicate rock outcrops. The acoustic intensity scale ranges from –31 to –13 dB. Scale bars represent 1 km, see Fig. 1 for the general location. *SB* sorted bedform; *dB* decibels; *Rocks* rock outcrops

a 22.5° azimuth. This lower scatter suggests a more consistent and well-defined hydrodynamic regime governing the orientation of bedforms in the Sines sector compared to the more variable conditions near the Sado estuary.

Geometric characterization through elongation, compactness, and rectangularity indices further distinguish the nature of these bedforms and their constituent types. Elongation index histograms indicate that most shapes are moderately elongated (Type B ISBs), with the Sines sector showing a higher degree of elongation than the Sado sector (Fig. S8 in the Supplementary Information). Compactness and rectangularity indices in both sectors follow negatively skewed distributions, with modal intervals of 0.7–0.8 for compactness (Fig. S9 in the Supplementary Information) and over 0.72 for rectangularity (Fig. S10 in the Supplementary Information), confirming that most shapes are elliptical or rectangular in nature. These findings are consistent with the prevalence of Type B ISBs, which tend to be more compact and symmetrical, whereas the less frequent, lower-index values correspond to the more irregular Type C ISBs.

Finally, the calculation of the centreline attribute and the analysis of geometric symmetry provide a detailed classification of the dominant forms (Fig. 7). Elliptical–asymmetrical shapes are the most prevalent, accounting for 51% and 49% of the Sado and Sines sectors respectively, followed by elliptical–symmetrical forms. While both sectors show a similar prevalence of symmetry, the Sado sector exhibits a slightly higher tendency for overall asymmetry across all shapes. As summarized in Fig. 8, these elliptical bedforms primarily correspond to the isolated mud crescents, in an anastomosed sandy environment of Type B ISBs, whereas the sinuous–asymmetrical and crescentic categories represent the more irregular ISBs Type C forms. This integrated geometric approach confirms that the continental mid-shelf is dominated by organized, albeit slightly asymmetrical, bedform patterns shaped by regional bottom currents.

Cross-sectional morphological analysis of sorted bedforms

The cross-sectional morphology and structure of the ISBs were examined using ultra-high-resolution seismic profiles, revealing a complex stratigraphy in both the Sado and Sines sectors. In the Sado sector (Fig. 9a; Fig. S12 in the Supplementary Information), four seismic units (U1 to U4) were identified, separated by discontinuities D1, D2, and D3. The basal bedrock unit (U1), likely of Miocene age, exhibits heterogeneous reflectors suggesting an ephemeral submarine channel system. This is overlain by unit U2, a prograding sequence with a maximum thickness of ~5 ms two-way-time (TWT), equivalent to ~4 m (assuming 1,500 m/s sound propagation velocity), while the subsequent unit U3 reaches a maximum thickness of ~6 ms (TWT), or ~5 m. The high facies variability in U3 suggests a sudden variation of depositional processes associated with different transgressive cycles of the paleo-Setúbal canyon (Fig. 1). The uppermost unit, U4, sits atop discontinuity D3, displaying transparent

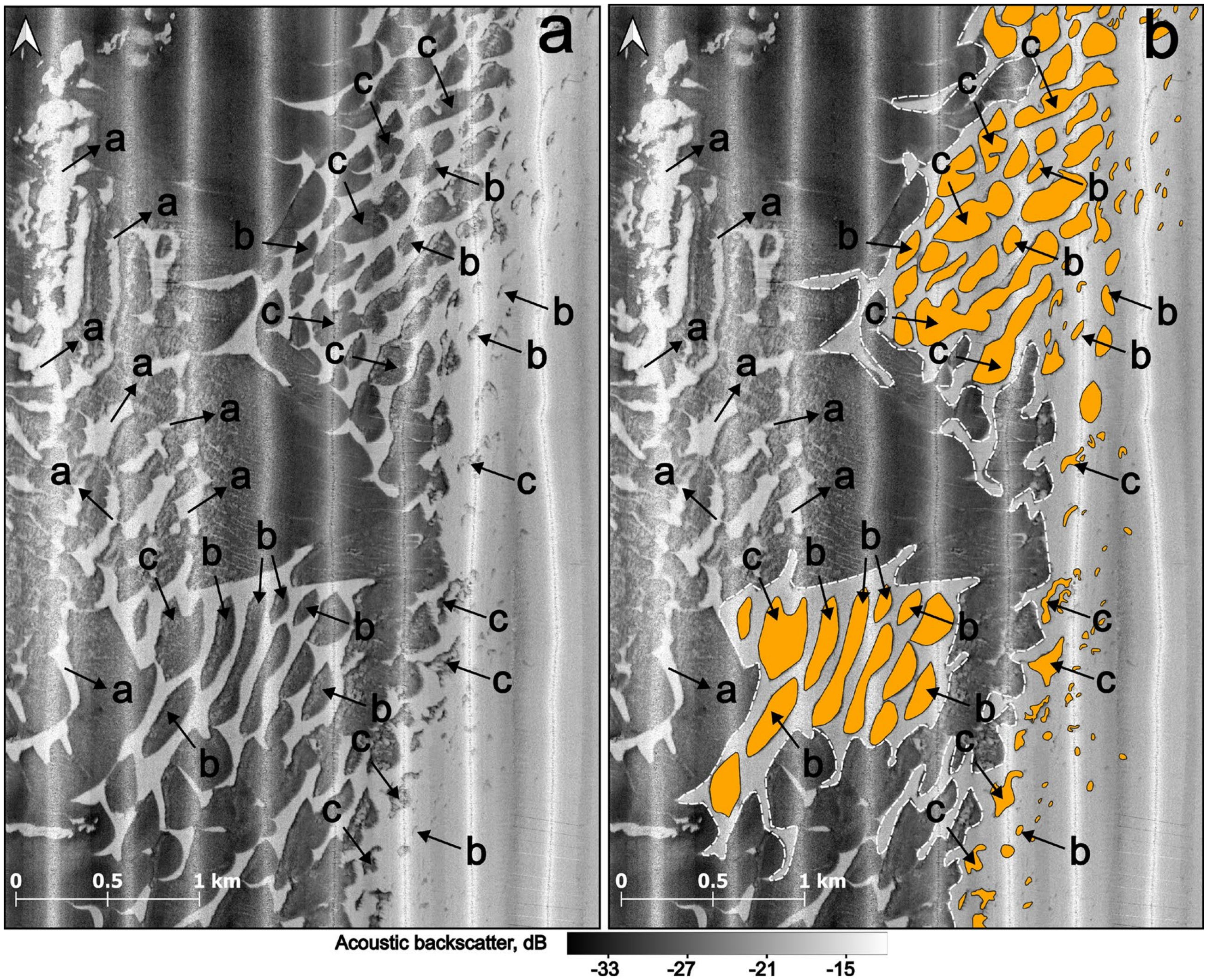

Fig. 5 Acoustic backscatter characterization of sorted bedforms in the Sines sector. **a** Backscatter mosaic illustrating the spatial distribution of the three identified sorted bedform (SB) types: Type A (**a**), Type B (**b**), and Type C (**c**). Fine sediments (low intensity, dark gray) dominate the seaward side, while coarse sediments (high intensity, light gray) are more prominent on the landward side. **b** Detailed interpretation of the sediment facies boundary (white dashed line), with Type B and Type C bedforms highlighted in solid orange for enhanced visualization. Dotted polygons indicate rock outcrops. The acoustic intensity scale ranges from –33 to –15 dB. Scale bars represent 1 km, see Fig. 1 for the general location. *SB* sorted bedform; *dB* decibels; *Rocks* rock outcrops

facies with a laminar geometry below ~105 ms (TWT) or ~78 m and a thickness of barely over ~1 ms (TWT), i.e., less than 1 m. Between ~105 ms and ~75 ms (TWT) or ~56 m, U4 develops the characteristic asymmetric morphology of the ISBs before thinning to less than ~0.5 ms (TWT) or ~0.6 m above ~75 ms (TWT) or ~56 m water depth.

In the Sines sector, the seismic architecture is characterized by five distinct units (U1 to U5) that reflect a history of paleo-valley infilling and subsequent bedform development (Fig. 9b; Fig. S13 in the Supplementary Information). The bedrock unit (U1), which is composed of folded Miocene strata, is incised by V-shaped paleo-valleys containing unit U2, which reaches a maximum thickness of ~13 ms (TWT) equivalent to ~10 m. The overlying unit U3 has a maximum thickness of ~3 ms (TWT) or ~2 m, while unit U4, which infills a paleo-valley, reaches up to 7 ms (TWT) or ~5 m. The most recent unit, U5, displays a dual character: to the east, it forms a landward-thickening retrogradational sequence, whereas to the west, it comprises the ISBs (sub-units U5a, U5b, and U5c). These ISBs, which become younger landwards, extend along the profile with a thickness varying from 0.75 ms to 1.5 ms (TWT) or ~0.5 m to ~1 m. Near the shelf break at ~160 ms (TWT) or ~120 m depth, the lateral equivalents of these units lose their ripple-like geometry and transition into a sub-horizontal aggradational structure. It is important to note that the unit designations (U1–U5) of the

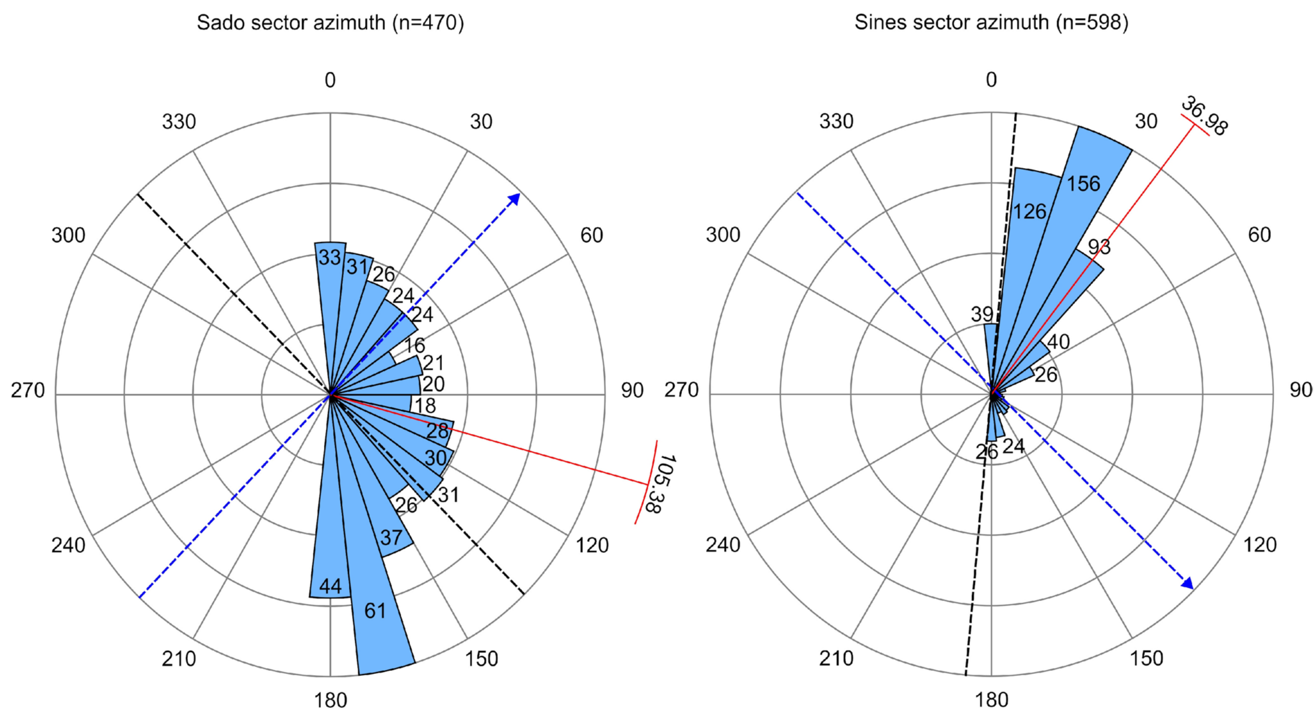

Fig. 6 Rose diagrams showing the azimuthal distribution (30° bins) of sorted bedform (SB) elongations (Types B and C). Left panel: Sado sector (*n*=470). Right panel: Sines sector (*n*=598). Black dashed lines indicate the local orientation of the bathymetric contours (isobaths). Red lines represent the mean azimuthal value of the SB elongations. Blue dashed arrows indicate the dominant wave directions. Note the significant data scatter in the Sado sector (left) compared to the Sines sector (right). The mean elongation direction is oriented near-perpendicular to the measured wave direction in the Sines sector and perpendicular to the main wave direction reported for the Sado sector by Brito (2009). *SB* sorted bedform; *n* number of observations

Sado and Sines sectors follow chronostratigraphic reflectors; despite lateral facies variations, such as progradation in the Sado sector versus infilling in the Sines sector, this consistent naming underscores that these deposits are contemporaneous and share the same regional stratigraphic position.

The integration of ultra-high-resolution seismic data with acoustic backscatter provides a definitive link between subsurface stratigraphy and seafloor texture across the study area. In the Sines sector, Type B ISBs are characterized by a clear sequence of asymmetric crests and troughs that progressively lose their regular profile as they disappear landward (Fig. 10). A similar relationship is observed in the Sado sector, where the correlation between seismic facies and backscatter highlights the morphological transition of the ISBs (Fig. S14 in the Supplementary Information).

Sediment analysis and correlation with backscatter data

The granulometric analyses of the unconsolidated seafloor sediments across the NACoS shelf reveal a composition predominantly consisting of slightly gravelly to gravelly sand (Fig. S15 and Table S5 in the Supplementary Information). Mean grain sizes vary between fine and very coarse sand, representing the critical coarse fraction required for the initiation and maintenance of the sorted bedforms. The fine sand samples (>2 φ) also contain a finer fraction (>4 φ) ranging from 3.9% to 7.8% (Table S5 in the Supplementary Information). This finer fraction was likely incorporated subsequently into the system through fall-out from suspension during lower-energy intervals. It is important to note, however, that these values likely underestimate the true mud content, as silts and clays were generally not retained by the sampling instrument. Despite this limitation, a linear correlation is observed in the bulk sediment, whereas the backscatter intensity more accurately reflects the actual grain-size distribution, which was likely enriched in the finer fractions that were washed out during the sampling procedure.

The integration of backscatter and sedimentological data provides a clear reconstruction of seabed sediment distribution patterns in both the Sado and Sines sectors. A strong correlation exists between acoustic backscatter and mean grain size, where lower intensities correspond to fine–medium sand and higher intensities represent very coarse–coarse sand (Fig. S15 in the Supplementary Information). Backscatter intensity histograms reveal bimodal distributions in both sectors; in the Sado sector, the modes are closer together, suggesting a more

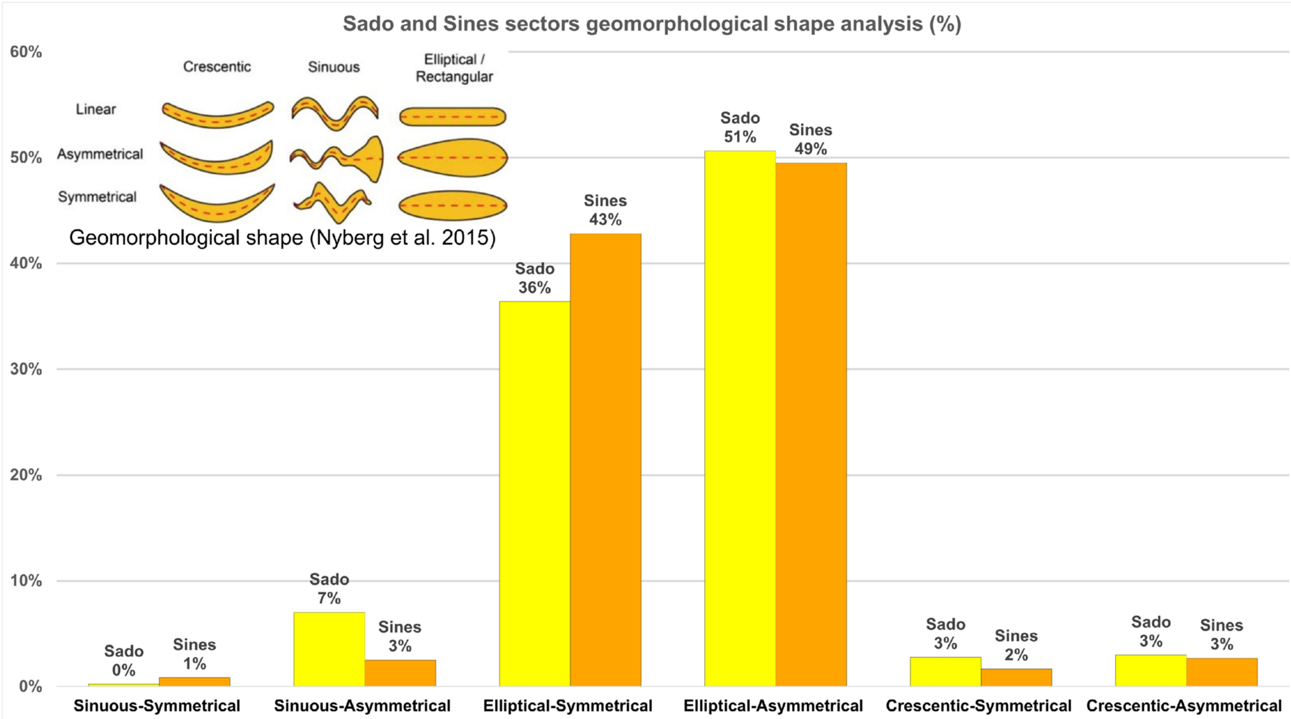

Fig. 7 Quantitative geomorphological shape analysis (%) of Type B and Type C sorted bedforms (SBs) in the Sado and Sines sectors. Yellow bars represent the Sado sector, and orange bars represent the Sines sector. The classification into crescentic, sinuous, and elliptical/rectangular shapes follows the conceptual framework of Nyberg et al. (2015), as illustrated in the upper-left inset. Note the high prevalence of elliptical–asymmetrical (49–51%) and elliptical–symmetrical (36–43%) shapes in both study areas, contrasting with the low frequency of sinuous and crescentic types

homogeneous sediment distribution, whereas in the Sines sector, the modes are better defined. In the latter sector, the primary mode (-22 dB) corresponds to the very coarse to coarse sand found in the ISB troughs (Types B and C) and sand stripes (Type A), whereas the secondary mode (-28 dB) represents the fine-to-medium-grained sands characteristic of the low-relief ISB types B and C. This acoustic differentiation confirms that backscatter intensity is an effective proxy for mapping the intricate textural variations of the mid-shelf depositional environments.

Discussion

The ISBs investigated in this study stimulated the following questions for discussion:

i) what environmental parameters conditioned the formation of the SBs?
ii) what is the age and present-day activity of the SBs?

Environmental control of the ISBs

The two groups of analyzed ISBs occur at minimum water depths of approximately −70 m and −100 m, locations that coincide with internal shelf breaks as detailed in Tables S1 and S2 in the Supplementary Information. The environmental setting of the ISBs is influenced by coastal winds—predominantly from the NW and SW in the Sado sector and from the NW in the Sines sector—and by southerly driven surface currents that run roughly parallel to the bathymetric contours (Fig. S2 in the Supplementary Information). Morphologically, the ISBs are low-relief features, not exceeding 1 m in height, which developed directly on top of a ravinement surface carved into a tectonized substratum ranging from Mesozoic to Pliocene sedimentary rocks (Fig. 9a, b). Sediment analyses confirm that the grain-size distribution of the two sectors is equivalent, with backscatter coverage indicating that these forms emerge at the transition from deep-water fine-grained sediments to shallower-water coarser-grained sediments.

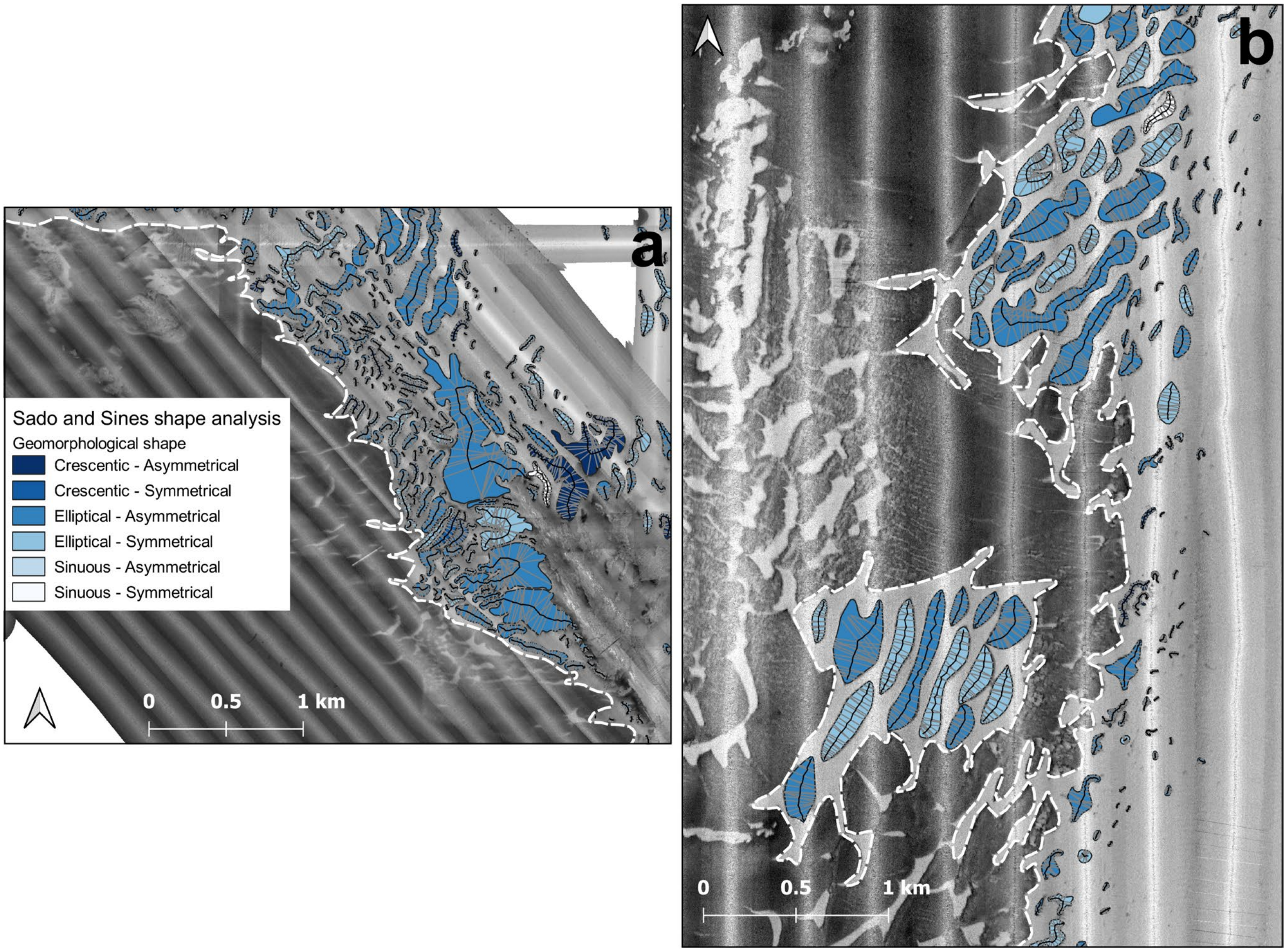

Fig. 8 Spatial distribution of sorted bedform (SB) geomorphological shape classes. **a** Sado sector backscatter mosaic overlaid with shape classification polygons. **b** Sines sector backscatter mosaic overlaid with shape classification polygons. Six shape classes (Crescentic, Elliptical, and Sinuous; Symmetrical/Asymmetrical) are identified following the quantitative methodology of Nyberg et al. (2015). The white dashed line delineates the acoustic facies boundary between finer sediments (low backscatter, dark gray) and coarser sediments (high backscatter, light gray). Scale bars represent 1 km, see Fig. 1 for the general location

Variations in shelf orientation and coastal topography further differentiate the two ISB groups. The shallower Sado sector group formed on an NW–SE trending segment, partially protected from NW winds by a ~600 m high mountain belt and subjected primarily to W to SW storms. In this area, the ISBs exhibit a large scatter in their elongation direction and are situated on a gently sloping platform (0.35° slope) at the foot of a steep, ~7 m high scarp. In contrast, the deeper Sines sector group lies on a segment fully exposed to north-westerly swells, where the elongation of the ISBs is perpendicular to the main wave direction. This sector is characterized by steeper inner-outer shelf breaks (0.97° to 1.23° slopes) compared to the Sado sector, with the ISBs forming on a 0.7° dipping surface at the foot of a 1.2° slope.

The observed orientation and dimensions of these features suggest they are shaped by wave-driven bottom currents. Although deep current measurements are not available, the data indicate transport directions parallel to dominant wave regimes, with the scatter in the Sado sector likely associated with the interference of north-westerly and south-easterly swells. The considerably longer ISBs in the Sines sector (Fig. S6 in the Supplementary Information), combined with its lack of topographical protection and greater water depths, suggest a regime of stronger and more directional bottom currents. Furthermore, the higher compactness coefficient in the Sado sector (Fig. S9 in the Supplementary Information) may result from the action of sub-perpendicular currents, whereas the single dominant current in the Sines sector enhances the linear shape of the bedforms.

Based on the availability of unconsolidated fine and coarse silts throughout the middle and outer shelf documented on the surficial sediment chart (Fig. S1 in the Supplementary Information), two non-mutually exclusive hypotheses for the formation of these ISBs can be

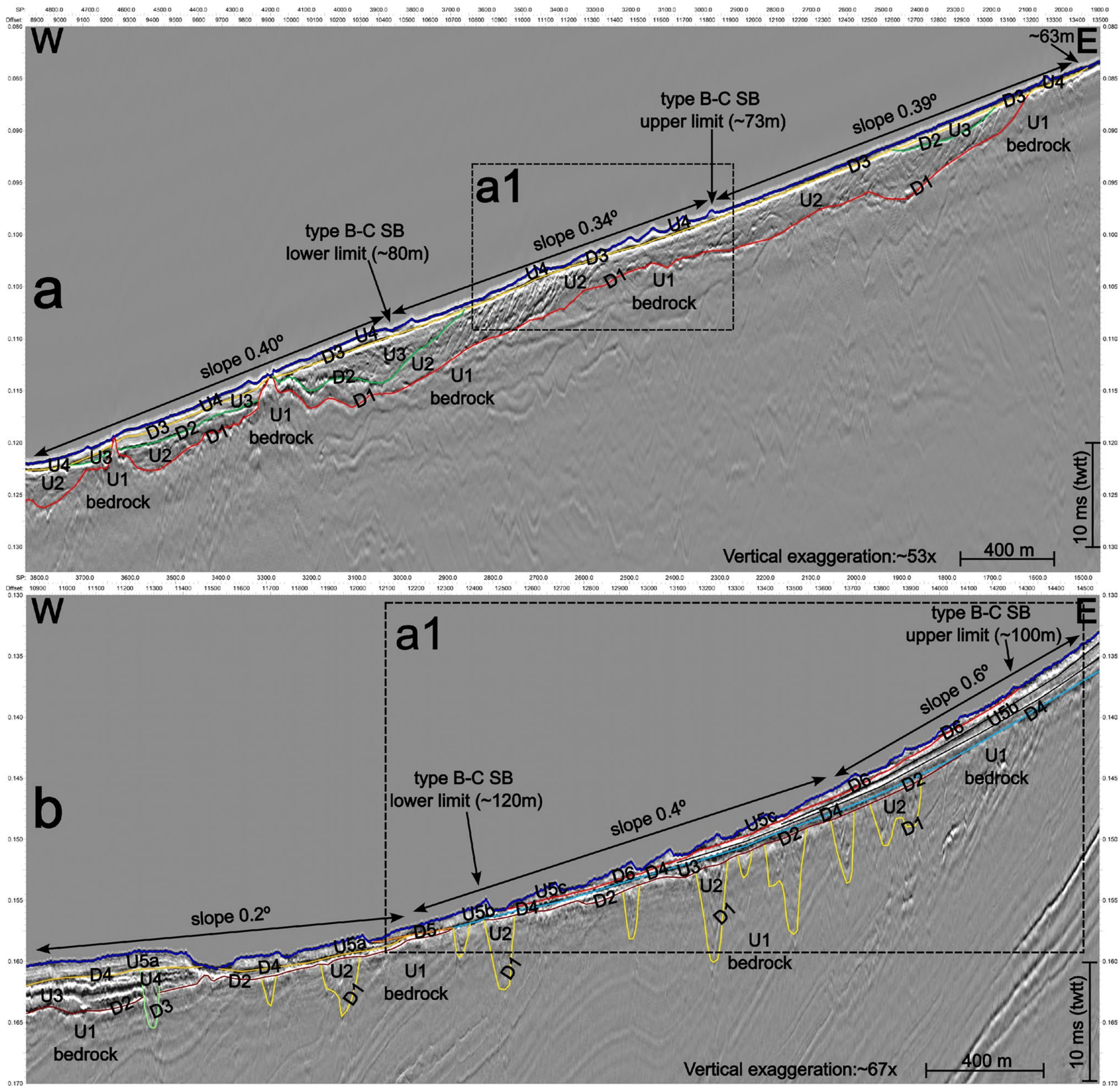

Fig. 9 Interpreted ultra-high-resolution seismic reflection profiles of the **a** Sado sector and **b** Sines sector. The West–East (W–E) transects illustrate the stratigraphic architecture from the acoustic U1 bedrock up to **a** the U4 seismic unit and **b** the U5c seismic unit. Major discontinuities and reflectors define the boundaries between the identified units, ranging from D1 to D3 in (**a**) [D1 (red), D2 (green), and D3 (yellow)] and from D1 to D6 in (**b**). Both profiles highlight the occurrence of Type B–C sorted bedforms (SB), with bathymetric limits ranging from **a** ~80 m (lower limit) to ~73 m (upper limit), and **b** ~120 m (lower limit) to ~100 m (upper limit). Seafloor slope gradients range from **a** 0.34° to 0.40° and **b** increase upslope from 0.2° to 0.6°. Dashed boxes **a1** indicate the location of detailed close-up views provided in (**a**) (Fig. S7 in the Supplementary Information) and **b** Fig. 10, see Fig. 1 for the general location. Horizontal scale bars represent 400 m; vertical scale is in 10 ms (TWTT). Vertical exaggeration is **a** ~53× and **b** ~67×. *SB* sorted bedform; *D* discontinuity/reflector; *U* seismic unit; *TWTT* two-way travel time

formulated: (i) the landward invasion of fine-grained sediments over a sandy substratum and (ii) the mobilization and re-deposition of sediments through grain sorting into ripple-like features. In several locations the asymmetry of the bedforms suggests upslope progradation onto coastal sand wedges that also lie on top of the same erosional unconformity (Fig. 8, Fig. 9, and Fig. 10). The study area is located on an open-ocean swell coast, where winter and summer

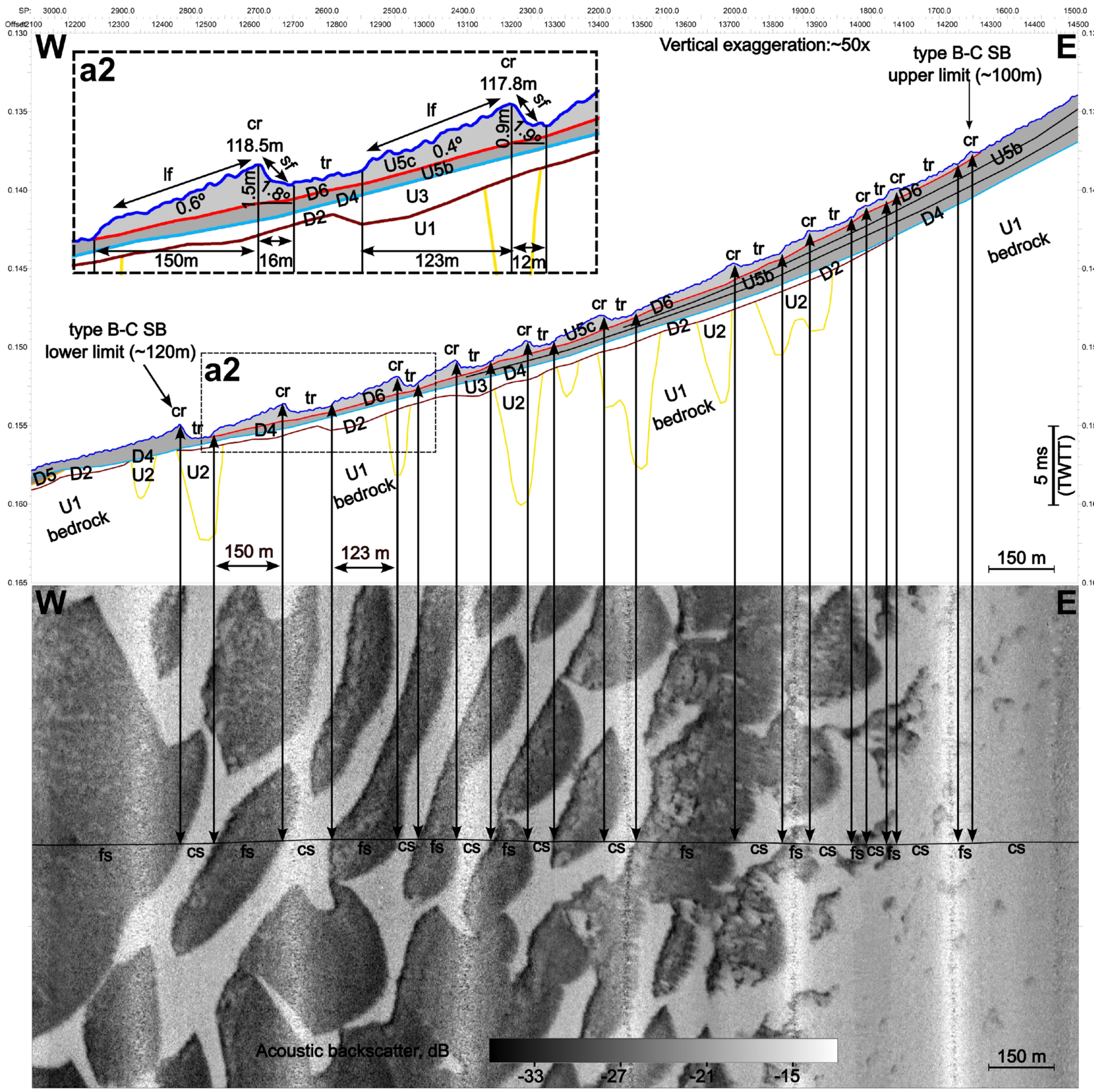

Fig. 10 Integrated seismic and acoustic characterization of type B–C sorted bedforms (see Fig. 1 for the location). The upper panel displays the stratigraphic architecture, where units U1 (bedrock), U2, U3, U5b, and U5c are identified, separated by reflectors D2, D4, and D6. The detailed inset (**a2**) shows the bedform morphology, including slope angles of the long (lf) and short (sf) flanks, heights (0.5–0.9 m), and crest-to-crest distances (117.8–118.5 m). Vertical arrows demonstrate the spatial correlation between sub-surface reflectors and seafloor acoustic facies. The vertical scale is shown in 5 ms two-way travel time (TWTT), and horizontal scale bars represent 150 m. Vertical exaggeration is ~50x. In the lower panel backscatter mosaic, fs denotes fine sediments (low backscatter) and cs denotes coarse sediments (high backscatter). See text for a detailed description. *SB* sorted bedform; *D* discontinuity/reflector; *U* seismic unit; *TWTT* two-way travel time; *cr* crest; *tr* trough; *lf* long flank; *sf* short flank; *cs* coarse sediment; *fs* fine sediment

fair-weather conditions differ considerably, acting upon a wide range of available grain sizes (Table S5 in the Supplementary Information). Under these conditions, the Effective Wave Base—defined as the depth at which siliciclastic sediment particles are mobilized on the seafloor—can vary significantly (Flemming 2024). According to this author, for example, 0.125 mm sands can be mobilized at water depths of 90 m by waves with a height of 4 m and a period of 12 s, leading to the formation of ripple-like bedforms. This active status is further supported by our estimated storm shear velocity of ~2.25 cm/s at 100 m depth. Based on the analytical thresholds reviewed in Flemming (2024), this shear stress exceeds the critical velocity required to mobilize grains up to ~1.0 mm (0 φ). Consequently, the local sediment spectrum (–1 to 4 φ) falls well within the active hydrodynamic domain during extreme storms, with coarser fractions undergoing bedload transport and finer fractions (>2 φ) easily reaching the threshold for suspended load. Given that the Effective Wave Base fluctuates according to wave dimensions during non-storm conditions, with wave heights between 3 m and 6 m consistently reaching the depth range of the ISBs in this study, the resulting seabed features exhibit a variety of shapes of different sorted bedforms. The outlines of the sorted bedforms range from sharp to fuzzy with superimposed patterns (Fig. 2 and Fig. 3), reflecting temporal variations in energy, wave orientation, and water depth changes throughout the last sea-level rise, i.e., post-Last Glacial Maximum.

Finally, the striking difference between the sediment patterns revealed by high-resolution backscatter and the surficial sediment chart underscores the limitations of discrete sampling. Traditional strategies, such as the 1-nautical-mile grid used by the Instituto Hidrográfico (1985) are unable to identify ISBs, because the sampling interval is larger than the features themselves (Fig. S1 in the Supplementary Information). Furthermore, it is worth noting that the ISBs are interrupted at both flanks of the Setúbal canyon, which suggests the possibility that southerly diverted upwelling currents hinder the formation of the ISBs in the vicinity of the canyon. Overall, these findings highlight that continuous geophysical mapping is essential to capture the true sedimentological complexity and hydrodynamic active zones of the continental shelf.

Age of the sorted bedforms

The study area features a continuous sand sheet extending from the present-day coastline to water depths typically between −30 and −50 m, reaching locally up to ~100 m (Fig. 1; Figs. S1 and S3 in the Supplementary Information). This sand sheet is inherently mobile across various timescales, as it is influenced by high-frequency processes, such as semi-diurnal tides, daily winds, and waves, as well as lower-frequency events, such as seasonal storms and long-term eustatic sea-level cycles. The stratigraphic analysis of seismic profiles reveals that the ISBs prograde over and overprint this coastal sand wedge at water depths of ~75 m and 100 m in the Sado and Sines sectors, respectively (Fig. 9 and Fig. 10; Fig. S14 in the Supplementary Information). Based on these observations and the analytical modeling by Flemming (2024), it is suggested that the ISBs remain active under present-day hydrodynamic conditions, although some features display diffuse boundaries or are overprinted by different depositional bodies (Fig. 4 and Fig. 5). It is here suggested that these patterns likely reflect variations in wave orientation and/or in the Effective Wave Base over time.

At the current scale of observation, it is evident that the ISBs have migrated shoreward, overlapping the coastal sand sheet deposits. This specific stratigraphic relationship indicates that the sand sheet deposits are older than the ISBs and likely represent relicts from periods of lower sea-level times. This upslope migration possibly resulted from significant shifts in hydrodynamic conditions triggered by the rapid sea-level rise after the Last Glacial Maximum. Consequently, we can argue that the relative ages of these features are intrinsically linked to the transgression, with the stratigraphic evidence suggesting a clear temporal succession, where the ISBs represent a more recent phase of sediment re-distribution.

Building on this stratigraphic framework, we can hypothesize about the initial age of ISB formation based on their depth and preservation state. It is proposed that the older SBs and ISBs are located at greater water depths, where they exhibit fuzzier outlines, while the younger, better-defined features lie at shallower depths. Assuming that ISB formation accompanied the eustatic sea-level rise, it is reasonable to conclude that the oldest and deepest bedforms—now at ~100 m depth—formed when the sea level was approximately 70 m above their current position. According to the eustatic curve, this corresponds to approximately 8.5 ky BP (Fig. 11). Thus, the distribution of these bedforms across the shelf serves as a morphological record of the post-glacial transgression over the last eight millennia.

Conclusions

The high-resolution geophysical and sedimentological data analysis from the SW Portuguese shelf demonstrates that ISBs are dynamic features that prograde landward from fine-grained domains toward the coastal sand sheet (wedge). This stratigraphic relationship, observed in both the Sado and Sines sectors, confirms a consistent pattern of upslope migration driven by the post-Last Glacial Maximum sea-level rise. The formation of these bedforms is fundamentally controlled by bottom current shear velocities, which are modulated not only by water depth but also by specific seafloor morphologies and shelf slope variations. Consequently, the ISBs serve as sensitive indicators of the hydrodynamic energy gradients present across the continental shelf.

The geometry and orientation of these features are further determined by the constancy and direction of the regional wave regime relative to the shelf slope. Our findings indicate that the influence of sub-perpendicular currents tends to generate shorter and more compact ISB shapes, whereas more directional regimes result in

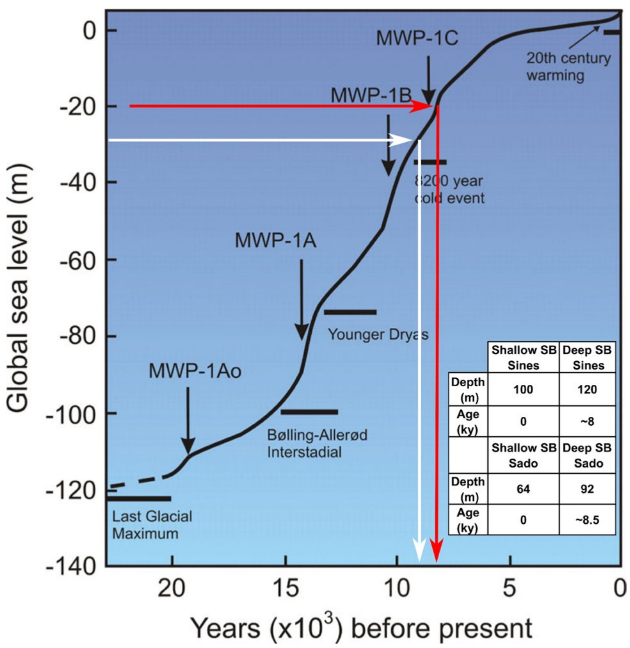

Fig. 11 Hypothesized age determination of sorted bedforms (SBs) by plotting the bathymetric range of each sector on the post-Last Glacial Maximum global sea-level curve. The curve illustrates major climatic events and meltwater pulses (MWP), including MWP-1Ao (~19.6–18.8 ky BP), MWP-1A (14.6–13.8 ky BP), MWP-1B (11.0–8.8 ky BP), and MWP-1C (~8.2–7.6 ky BP), adapted from Gornitz (2013). The inset table summarizes the shallow and deep limits of SBs in the Sines and Sado sectors. The red and white arrows represent the ~20 m (Sines) and ~28 m (Sado) bathymetric differences, respectively, projected onto the curve to estimate the temporal window of bedform development and preservation. See text for a detailed discussion. *MWP* meltwater pulse; *ky BP* thousand years before present; *SB* sorted bedform

elongated forms. Stratigraphic evidence and analytical modeling suggest that these processes initiated approximately 8.5 ka BP during the post-glacial transgression, under the persistent influence of wind-controlled alongshore currents. This temporal framework highlights that the ISBs are not relict features but have been actively evolving throughout the Holocene.

Finally, this study underscores the critical importance of continuous mapping techniques in shelf environments. Because the dimensions of the ISBs are smaller than the sampling intervals used in traditional sediment charts, discrete sampling strategies are unable to resolve these bedforms or the complex grain-size variations associated with them. By overcoming these resolution limits, this work demonstrates that the mid-shelf is a highly heterogeneous and hydrodynamically active zone. Ultimately, these results provide a new model for understanding sediment partitioning and sorted bedform evolution on sediment-starved margins during periods of sea-level rise.

Supplementary Information The online version contains supplementary material available at https://doi.org/10.1007/s00531-026-02594-7.

Acknowledgements We acknowledge MINEPLAT project ALT20-03-0145-FEDER-000013 that funded the acquisition of the data presented in this paper. We acknowledge Marine Geology and Geophysics Laboratory (SEISLAB) at Instituto Português do Mar e da Atmosfera, I.P. (IPMA, I.P.) for access to the facilities and software tools that were used in the interpretation of the data presented in this paper. Projects MARE - Marine and Environmental Sciences Centre, Reference: UID/04292/2025, https://doi.org/10.54499/UID/04292/2025 and IDL—Instituto Dom Luiz, Reference: UID/PRR2/50019/2025, DOI https://doi.org/10.54499/UID/PRR2/50019/2025. We express our sincere gratitude to the anonymous reviewers for their insightful feedback and academic commitment. Their constructive review challenged and refined our analysis, significantly strengthening the final version of this manuscript.

Funding Open access funding provided by FCT|FCCN (b-on).

Data availability All primary data generated during this study are included in this published article and its supplementary informationfiles, while the complete underlying datasets are openly available in the Zenodo repository under reference https://doi.org/10.5281/zenodo.20829574.

References

Blott SJ, Pye K (2001) GRADISTAT: a grain size distribution and statistics package for the analysis of unconsolidated sediments. Earth Surf Process Landf 26:1237–1248. https://doi.org/10.1002/esp.261

Brasebin M, Perret J, Matelier R, Thomas B (2019) NeatMap—QGIS Python Plugins Repository. Available via https://plugins.qgis.org/plugins/NeatMap/. Accessed 29 June 2023

Brito P (2009) Impactos da elevação do nível médio do mar em ambientes costeiros: o caso do estuário do Sado. PhD Thesis, Universidade de Lisboa, Lisboa

Cacchione DA, Drake DE, Grant WD, Tate GB (1984) Rippled scour depressions on the inner continental shelf off central California. J Sediment Res 54:1280–1291. https://doi.org/10.1306/212F85BC-2B24-11D7-8648000102C1865D

Costa M, Esteves R (2009) Clima de agitação marítima na costa oeste de Portugal Continental. In: Proceedings of XI Jornadas Técnicas de Engenharia Naval - O Sector Marítimo Português. Instituto Superior Técnico, Lisboa, pp 413–426

Costa M, Silva R, Vitorino J (2001) Contribuição para o estudo do clima de agitação marítima na costa portuguesa. In: Proceedings of 2ª Jornadas de Engenharia Costeira e Portuária. Associação Nacional de Navegação, Sines, p 20

Diesing M, Kubicki A, Winter C, Schwarzer K (2006) Decadal scale stability of sorted bedforms, German Bight, southeastern North Sea. Cont Shelf Res 26:902–916. https://doi.org/10.1016/j.csr.2006.02.009

Duarte H, Wardell N, Monrigal O (2017) Advanced processing for UHR3D shallow marine seismic surveys. Surf Geophys 15:347–358. https://doi.org/10.3997/1873-0604.2017022

EMODnet Bathymetry Consortium (2022) EMODnet Digital Bathymetry (DTM 2022). EMODnet Bathymetry. https://sextant.ifremer.fr/geonetwork/srv/api/records/ff3aff8a-cff1-44a3-a2c8-1910bf109f85. Accessed 26 Mar 2023

Farr TG, Rosen PA, Caro E et al (2007) The shuttle radar topography mission. Rev Geophys 45:RG2004. https://doi.org/10.1029/2005RG000183

Flemming BW (2024) The concept of wave base: fact and fiction. Geo-Mar Lett 44:14. https://doi.org/10.1007/s00367-024-00776-3

Folk RL (1954) The distinction between grain size and mineral composition in sedimentary-rock nomenclature. J Geol 62:344–359. https://doi.org/10.1086/626171

GEBCO Bathymetric Compilation Group (2022) GEBCO_2022 Grid. Br Oceanogr Data Cent. https://www.bodc.ac.uk/data/published_data_library/catalogue/10.5285/e0f0bb80-ab44-2739-e053-6c86abc0289c. Accessed 26 Mar 2023

Goff JA, Mayer LA, Traykovski P et al (2005) Detailed investigation of sorted bedforms, or "rippled scour depressions", within the Martha's Vineyard Coastal Observatory, Massachusetts. Cont Shelf Res 25:461–484. https://doi.org/10.1016/j.csr.2004.09.019

Instituto Hidrográfico (1985) Carta dos sedimentos superficiais da plataforma continental: Folha 5—Cabo da Roca ao Cabo de Sines, escala 1:150 000. Instituto Hidrográfico, Lisboa, Lisboa

Liu H, Wang L, Sherman D et al (2010) An object-based conceptual framework and computational method for representing and analyzing coastal morphological changes. Int J Geogr Inf Sci 24:1015–1041. https://doi.org/10.1080/13658810903270569

Liu S, Goff JA, Flood RD et al (2018) Sorted bedforms off Western Long Island, New York, USA: asymmetrical morphology and twelve-year migration record. Sedimentology 65:2202–2222. https://doi.org/10.1111/sed.12462

Lo Iacono C, Guillén J (2008) Environmental conditions for gravelly and pebbly dunes and sorted bedforms on a moderate-energy inner shelf (Marettimo Island, Italy, western Mediterranean). Cont Shelf Res 28:245–256. https://doi.org/10.1016/j.csr.2007.08.005

Mil-Homens M, Brito P, Magalhães V et al (2022) Integrated geophysical and sedimentological datasets for assessment of offshore borrow areas: the CHIMERA project (western Portuguese coast). Geol Soc Lond Spec Publ 505:131–153. https://doi.org/10.1144/SP505-2019-100

Murray AB, Thieler ER (2004) A new hypothesis and exploratory model for the formation of large-scale inner-shelf sediment sorting and "rippled scour depressions." Cont Shelf Res 24:295–315. https://doi.org/10.1016/j.csr.2003.11.001

Neres M, Neves MC, Custódio S et al (2018) Gravitational potential energy in Iberia: a driver of active deformation in high-topography regions. J Geophys Res Solid Earth 123:10277–10296. https://doi.org/10.1029/2017JB015002

Nyberg B, Buckley SJ, Howell JA, Nanson RA (2015) Geometric attribute and shape characterization of modern depositional elements: a quantitative GIS method for empirical analysis. Comput Geosci 82:191–204. https://doi.org/10.1016/j.cageo.2015.06.003

QGIS Development Team (2023) QGIS Geographic Information System. QGIS Association, Graubünden, Switzerland. Available via https://www.qgis.org Accessed 20 June 2023

Rebêlo L, Ferraz M, Brito P, Terrinha P (2012) Quantification of sediments accumulated in the NW sector of Tróia Peninsula (Portugal) between 1928 and 1995. J Coast Conserv 16:261–268. https://doi.org/10.1007/s11852-011-0171-2

Swift DJP, Field ME (1981) Evolution of a classic sand ridge field: Maryland sector, North American inner shelf. Sedimentology 28:461–482. https://doi.org/10.1111/j.1365-3091.1981.tb01695.x

Terrinha P, Duarte H, Brito P et al (2019) The Tagus River delta landslide, off Lisbon, Portugal Implications for marine geo-hazards. Mar Geol 416:105983. https://doi.org/10.1016/j.margeo.2019.105983

Udden JA (1914) Mechanical composition of clastic sediments. GSA Bull 25:655–744. https://doi.org/10.1130/GSAB-25-655

Vitorino J, Oliveira A, Jouanneau JM, Drago T (2002) Winter dynamics on the northern Portuguese shelf. Part 1: physical processes. Prog Oceanogr 52:129–153. https://doi.org/10.1016/S0079-6611(02)00003-4

Wentworth CK (1922) A scale of grade and class terms for clastic sediments. J Geol 30:377–392. https://doi.org/10.1086/622910

Xing F, Wang YP, Wang HV (2012) Tidal hydrodynamics and fine-grained sediment transport on the radial sand ridge system in the southern Yellow Sea. Mar Geol 291–294:192–210. https://doi.org/10.1016/j.margeo.2011.06.006